Permutation entropy based time series analysis: Equalities in the input signal can lead to false conclusions

Zunino, Luciano ; Olivares, Felipe ; Scholkmann, Felix ; Rosso, Osvaldo A

DOI: https://doi.org/10.1016/j.physleta.2017.03.052

Post-print. Original version: Zunino, L., Olivares, F., Scholkmann, F., Rosso, O. A. (2017). Permutation entropy based time series analysis: Equalities in the input signal can lead to false conclusions. *Physics Letters A*, **281** (22), 1883-1892.

Permutation entropy based time series analysis: Equalities in the input signal can lead to false conclusions

Luciano Zunino [a,b,*], Felipe Olivares [c], Felix Scholkmann [d,e], Osvaldo A. Rosso [f,g,h]

[a] *Centro de Investigaciones Ópticas (CONICET La Plata – CIC), C.C. 3, 1897 Gonnet, Argentina*
[b] *Departamento de Ciencias Básicas, Facultad de Ingeniería, Universidad Nacional de La Plata (UNLP), 1900 La Plata, Argentina*
[c] *Instituto de Física, Pontificia Universidad Católica de Valparaíso (PUCV), 23-40025 Valparaíso, Chile*
[d] *Research Office for Complex Physical and Biological Systems (ROCoS), Mutschellenstr. 179, 8038 Zurich, Switzerland*
[e] *Biomedical Optics Research Laboratory, Department of Neonatology, University Hospital Zurich, University of Zurich, 8091 Zurich, Switzerland*
[f] *Instituto de Física, Universidade Federal de Alagoas (UFAL), BR 104 Norte km 97, 57072-970, Maceió, Alagoas, Brazil*
[g] *Instituto Tecnológico de Buenos Aires (ITBA) and CONICET, C1106ACD, Av. Eduardo Madero 399, Ciudad Autónoma de Buenos Aires, Argentina*
[h] *Complex Systems Group, Facultad de Ingeniería y Ciencias Aplicadas, Universidad de los Andes, Av. Mons. Álvaro del Portillo 12.455, Las Condes, Santiago, Chile*

ARTICLE INFO

Article history:
Received 8 February 2017
Received in revised form 29 March 2017
Accepted 30 March 2017
Available online 4 April 2017
Communicated by C.R. Doering

Keywords:
Time series analysis
Permutation entropy
Equalities
Spurious temporal correlations

ABSTRACT

A symbolic encoding scheme, based on the ordinal relation between the amplitude of neighboring values of a given data sequence, should be implemented before estimating the permutation entropy. Consequently, equalities in the analyzed signal, *i.e.* repeated equal values, deserve special attention and treatment. In this work, we carefully study the effect that the presence of equalities has on permutation entropy estimated values when these ties are symbolized, as it is commonly done, according to their order of appearance. On the one hand, the analysis of computer-generated time series is initially developed to understand the incidence of repeated values on permutation entropy estimations in controlled scenarios. The presence of temporal correlations is erroneously concluded when true pseudorandom time series with low amplitude resolutions are considered. On the other hand, the analysis of real-world data is included to illustrate how the presence of a significant number of equal values can give rise to false conclusions regarding the underlying temporal structures in practical contexts.

1. Introduction

Permutation entropy (PE) is becoming a popular tool for the characterization of complex time series. Since its introduction almost fifteen years ago by Bandt and Pompe (BP) in their foundational paper [1], it has been successfully applied in a wide range of scientific areas and for a vast number of purposes. Without being exhaustive, applications in heterogeneous fields, such as biomedical signal processing and analysis [2–10], optical chaos [11–15], hydrology [16–18], geophysics [19–21], econophysics [22–25], engineering [26–29], and biometrics [30] can be mentioned. The PE is just the celebrated Shannon entropic measure evaluated using the ordinal scheme introduced by BP to extract the probability distribution associated with an input signal. This ordinal symbolic method, based on the relative amplitude of time series values, naturally arises from the time series (without any model assumptions) and inherits the causal information that stems from the temporal structure of the system dynamics. The relative frequencies of ordinal or permutation patterns, that quantify the temporal ranking information in the data sequence, need to be firstly calculated. Because of its definition via ordinal relationships, the way to handle equal amplitude values may have significant consequences when estimating the ordinal patterns probability distribution. In the case of variables with continuous distributions, ties can be simply ignored because they are very rare. However, experimental data digitized with relatively low amplitude resolutions could have a non-negligible number of equalities and, consequently, the PE estimations may be significantly affected by the procedure to consider them. Equal values in the time series are very usually ranked according to their temporal order. The other recipe, suggested by BP [1], is to break ties by adding a small amount of noise. This second alternative has been rarely implemented. In this paper, we characterize the effect that the presence of equalities in the data sequence has on the PE estimations when the former, most used, approach is adopted. Through numerical and real-world data analysis, we demonstrate that the PE estimated values are biased

* Corresponding author at: Centro de Investigaciones Ópticas (CONICET La Plata – CIC), C.C. 3, 1897 Gonnet, Argentina.
E-mail addresses: lucianoz@ciop.unlp.edu.ar (L. Zunino), olivaresfe@gmail.com (F. Olivares), Felix.Scholkmann@gmail.com (F. Scholkmann), oarosso@gmail.com (O.A. Rosso).

http://dx.doi.org/10.1016/j.physleta.2017.03.052

as a consequence of the presence of equal values, and more regular dynamics than those expected can be erroneously concluded. We consider that this finding is relevant for a more appropriate interpretation of the results obtained when the PE is used for characterizing the underlying dynamics of experimentally acquired observables. In particular, the effect of ties should be especially considered when using the PE for comparing the regularity degree of two or more experimental datasets digitized with different amplitude resolutions. Our main motivation is to warn future PE users about the importance to take this limitation into account for avoiding potential misunderstandings. Obviously, all related quantifiers estimated using the BP symbolic representation, *i.e.* with the symbolic method that considers the temporal ranking information (ordinal or permutation patterns) of the time series, can be also affected by this issue. We can enumerate permutation statistical complexity [31,32], permutation directionality index [33], symbolic transfer entropy [34], Tsallis permutation entropy [35], Rényi permutation entropy [36,37], conditional entropy of ordinal patterns [38], permutation min-entropy [39], multiscale permutation entropy measures [40], permutation Hurst exponent estimator [41] and time-scale independent permutation entropy [42], among many others. It is worth mentioning here that Bian et al. [43] have proposed the *modified* permutation-entropy (mPE) as an interesting alternative for dealing with equal values. Mapping equal values to the same symbols, these authors have shown that the mPE allows for an improved characterization of heart rate variability signals under different physiological and pathological conditions. However, Bian and co-authors' approach has a different physical interpretation and can not be considered as a *generalized* permutation entropy. For instance, the mPE does not reach its maximum value for a totally random signals (white noise) as this actually happens for the standard PE. Also the *weighted* permutation entropy (WPE) has been introduced by Fadlallah et al. [44] a couple of years ago as an improved PE by incorporating amplitude information. Through this weighted scheme, better noise robustness and distinctive ability to characterize data with spiky features or having abrupt changes in magnitude have been achieved. As it will be shown below, the presence of ties also has a significant incidence on WPE estimated values.

The remainder of the paper is organized as follows. In Section 2, the PE is introduced. A testbed analysis on computer-generated time series is included in Section 3 in order to understand the incidence of the presence of equal values on the PE estimations. Section 4 presents a couple of applications to illustrate this drawback in practical situations. Finally, in Section 5, the main conclusions reached in this work are summarized.

2. Permutation entropy

The PE has been introduced by BP as a natural complexity measure for time series [1]. It is the Shannon entropy of the ordinal symbolic representation obtained from the original sequence of observations. The idea behind ordinal pattern analysis is to consider order relations between values of time series instead of the values themselves. This ordinal symbolization is distinguished from other symbolic representations principally due to important practical advantages. Namely, it is conceptually simple, computationally fast, robust against noise, and invariant with respect to nonlinear monotonous transformations. Furthermore, the BP ordinal method of symbolization naturally arises from the time series, avoids amplitude threshold dependencies that affect other more conventional symbolization recipes based on range partitioning [45], and, perhaps more importantly, inherits the causal information that stems from the dynamical evolution of the system. As stated by Amigó et al. [46], "ordinal patterns are not symbols *ad hoc* but they actually encapsulate qualitative information about the temporal structure of the underlying data." Because of all these advantages, the BP approach has been commonly implemented for revealing the presence of subtle temporal correlations in time series [39,47–54].

Next, we summarize how to estimate the PE from a time series with a toy numerical example. Let us assume that we start with the time series $X = \{4, 1, 6, 5, 10, 7, 2, 8, 9, 3\}$. To symbolize the series into ordinal patterns, two parameters, the *embedding dimension* $D \geq 2$ ($D \in \mathbb{N}$, number of elements to be compared with each other) and the *embedding delay* τ ($\tau \in \mathbb{N}$, time separation between elements) should be chosen. The time series is then partitioned into subsets of length D with delay τ similarly to phase space reconstruction by means of time-delay-embedding. The elements in each new partition (of length D) are replaced by their ranks in the subset. For example, if we set $D = 3$ and $\tau = 1$, there are eight different three-dimensional vectors associated with X. The first one $(x_0, x_1, x_2) = (4, 1, 6)$ is mapped to the ordinal pattern (102). The second three-dimensional vector is $(x_0, x_1, x_2) = (1, 6, 5)$, and (021) will be its related permutation. The procedure continues so on until the last sequence, $(8, 9, 3)$, is mapped to its corresponding motif, (120). Afterward, an ordinal pattern probability distribution, $P = \{p(\pi_i), i = 1, \ldots, D!\}$, can be obtained from the time series by computing the relative frequencies of the $D!$ possible permutations π_i. Continuing with the toy example: $p(\pi_1) = p(012) = 1/8$, $p(\pi_2) = p(021) = 1/4$, $p(\pi_3) = p(102) = 3/8$, $p(\pi_4) = p(120) = 1/8$, $p(\pi_5) = p(201) = 0$, and $p(\pi_6) = p(210) = 1/8$. The PE is just the Shannon entropy estimated by using this ordinal pattern probability distribution, $S[P] = -\sum_{i=1}^{D!} p(\pi_i)\log(p(\pi_i))$. Coming back to the example, $S[P(X)] = -(3/8)\log(3/8) - (1/4)\log(1/4) - 3(1/8)\log(1/8) \approx 1.4942$. It quantifies the *temporal structural diversity* of a time series. If some ordinal patterns appear more frequently than others, the PE decreases, indicating that the signal is less random and more predictable. This allows to unveil hidden temporal information that helps to achieve a better understanding of the underlying mechanisms that govern the dynamics. Technically speaking, the ordinal pattern probability distribution P is obtained once we fix the embedding dimension D and the embedding delay time τ. Taking into account that there are $D!$ potential permutations for a D-dimensional vector, the condition $N \gg D!$, with N the length of the time series, must be satisfied in order to obtain a reliable estimation of P [55,56]. For practical purposes, BP suggest in their seminal paper to estimate the frequency of ordinal patterns with $3 \leq D \leq 7$ and embedding delay $\tau = 1$ (consecutive points). It has been recently shown that the analysis of the PE as a function of τ may be particularly helpful for characterizing experimental time series on a wide range of temporal scales [32,57]. By changing the value of the embedding delay τ different time scales are being considered because τ physically corresponds to multiples of the sampling time of the signal under analysis. For further details about the BP methodology, we recommend Refs. [57–59]. It is common to normalize the PE, and therefore in this paper, a normalized PE given by

$$\mathcal{H}_S[P] = S[P]/S_{\max} = S[P]/\log(D!) \tag{1}$$

is implemented, with $S_{\max} = \log(D!)$ the value obtained from an equiprobable ordinal pattern probability distribution. Defined in this way, $\mathcal{H}_S$ ranges between 0 and 1. The maximum value is obtained for a totally random stochastic process (white noise) while the minimum value is reached for a completely regular (monotonically increasing or decreasing) time series.

Since the BP approach symbolizes the series replacing the observable value by its corresponding rank in the sequence, the occurrence of equal values deserves a special handle. In the case of two elements in the vector having the same value, they are very often ranked by their temporal order. For example, a vector $(1, 4, 1)$, would be mapped to (021). This is the most com-

monly implemented recipe for dealing with ties. Another alternative, much more rarely used, is to add a small amount of observational noise to break equalities. The amplitude of the noise should be sufficiently small to not modify the ordinal relations in the data set, except for those vectors which have equal values. We insist on the fact that this latter approach has been applied in very few cases. We can cite Refs. [41,53,54,60] as some of these rare exceptions. To the best of our knowledge, how the PE estimated values are affected by the occurrence of a high frequency of equal values in the original data has not been previously explored in detail. In an effort to fill this gap, we have included in the following two sections numerical and experimental tests for characterizing this PE limitation when equal values are ranked according to their order of appearance.

3. Numerical tests

To illustrate the effect that the occurrence of a high frequency of ties has on PE estimated values, we have numerically generated an ensemble of one hundred independent sequences of $N = 1{,}000$ pseudorandom integer values drawn from a discrete uniform distribution on the interval $[0, i]$ with i ranging from 1 to 50 with step equal to one. The MATLAB function *randi* has been used for such a purpose. For more information about this function, we refer the interested reader to the following website: www.mathworks.com/help/matlab/ref/randi.html. In particular, when $i = 1$, pseudorandom uniform binary sequences of 0's and 1's are considered. Examples of these pseudorandom uniform discrete time series for $i = 1$, $i = 9$, and $i = 50$ are plotted in Fig. 1. Obviously, the number of ties is very large for the binary case, and it decreases as i increases.

The normalized PE (Eq. (1)) with different embedding dimensions, $D \in \{3, 4, 5, 6\}$, and embedding delay $\tau = 1$ (consecutive data points) has been estimated for the one hundred independent realizations for each i-value. Mean and standard deviation (displayed as error bars) are shown in Fig. 2 as a function of i. The normalized PE estimated values associated with continuous uniformly distributed pseudorandom numbers on the open interval $(0, 1)$, generated by implementing the *rand* function of MATLAB with a Mersenne Twister generator algorithm [61], have been also included. Being more precise, means from one hundred independent realizations of the same length ($N = 1{,}000$) for the different embedding dimension are indicated with horizontal dashed lines. It is clearly observed that normalized PE values from pseudorandom discrete time series with a high frequency of occurrence of equal values are much lower than those obtained for a pseudorandom continuous time series, leading to a totally spurious identification of non-random temporal structures. Because of the way ties are ordered, the relative frequencies of some permutation patterns are overestimated in detriment of those associated with other motifs which are underestimated, and, consequently, a non-uniform ordinal pattern probability distribution is obtained. This causes a decrease in the normalized PE estimation that could be erroneously interpreted as a signature of temporal correlation. Estimated PE values for the pseudorandom discrete simulations converge to those calculated for the pseudorandom continuous counterparts as the i-value increases. Analysis by implementing the WPE have been also carried out. For further details about this different definition of PE, that retains amplitude information, please see Ref. [44]. Results obtained, shown in Fig. 3, confirm that this improved ordinal permutation quantifier also suffers from this weakness.

As it is observed in Fig. 4, we have found qualitative similar findings for larger time series ($N = 10{,}000$ data points). Actually, the rate of convergence of the normalized PE estimations from the discrete to the continuous case is slower when longer time series are considered (please compare enlargements of Figs. 2 and 4). Besides, in another numerically controlled test, pseudorandom sequences of continuous (uniform, normal and exponential) distributions have been discretized and analyzed. Behavior observed are qualitatively equivalent, *i.e.* once again the PE estimations decrease when the number of discretization levels decreases, suggesting (in-

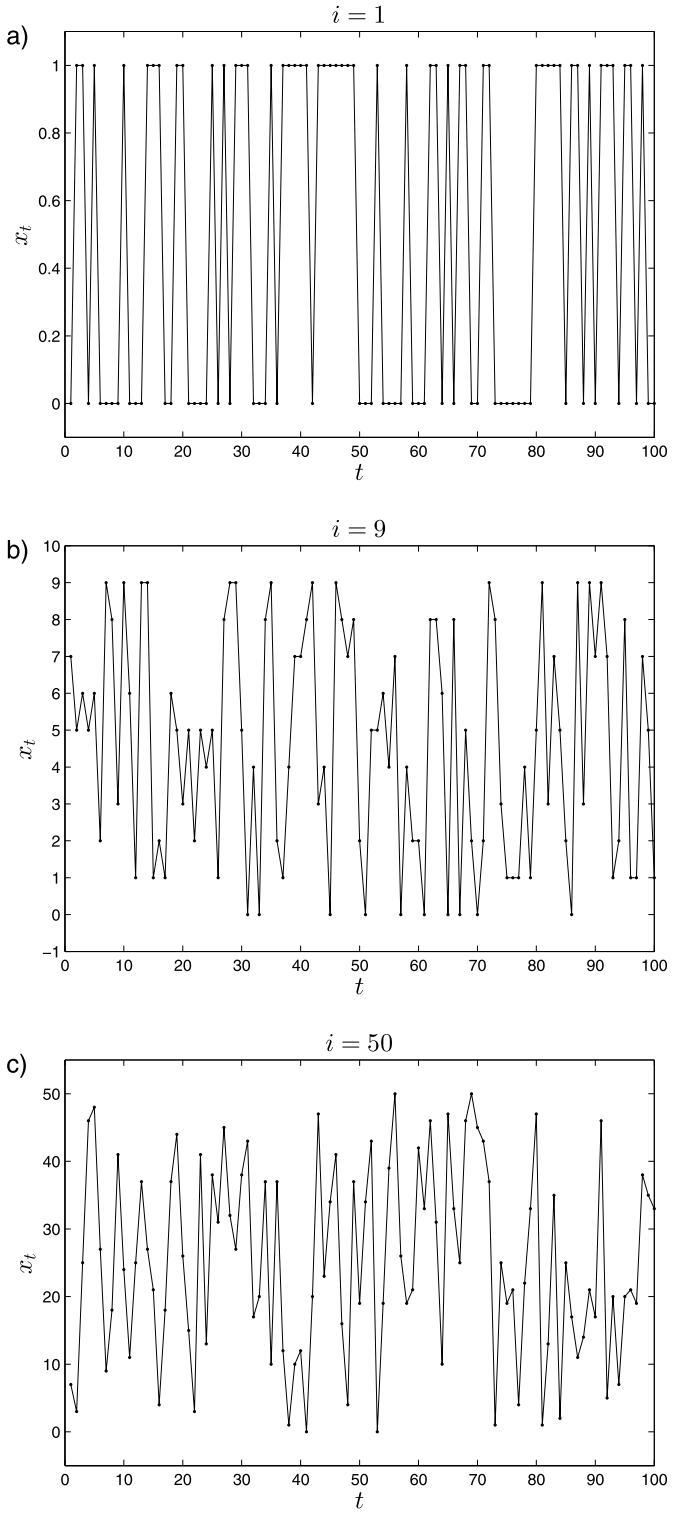

Fig. 1. Some examples of the numerically generated discrete pseudorandom sequences. Integer values are pseudorandomly drawn from a discrete uniform distribution on the interval $[0, i]$ with a) $i = 1$, b) $i = 9$, and c) $i = 50$. Only one hundred data points are depicted for a better visualization.

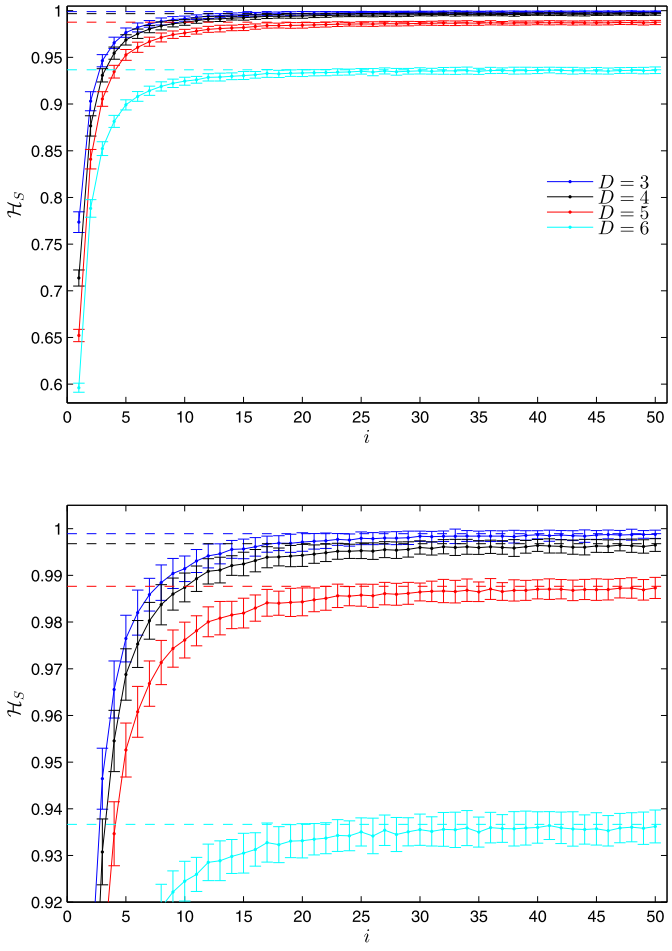

Fig. 2. Top: Mean and standard deviation (displayed as error bars) of $\mathcal{H}_S$ (Eq. (1)) for one hundred independent realizations of $N = 1{,}000$ pseudorandom integer values drawn from a discrete uniform distribution on the interval $[0, i]$. Results obtained for different embedding dimensions ($D \in \{3, 4, 5, 6\}$) and embedding delay $\tau = 1$ are included. Horizontal dashed lines indicate the mean value of $\mathcal{H}_S$ for one hundred independent realizations of $N = 1{,}000$ pseudorandom numbers from a continuous uniform distribution on the open interval $(0, 1)$. Bottom: Enlargement for a better view of the results obtained for lower discretization (larger values of i). (For interpretation of the references to color in this figure legend, the reader is referred to the web version of this article.)

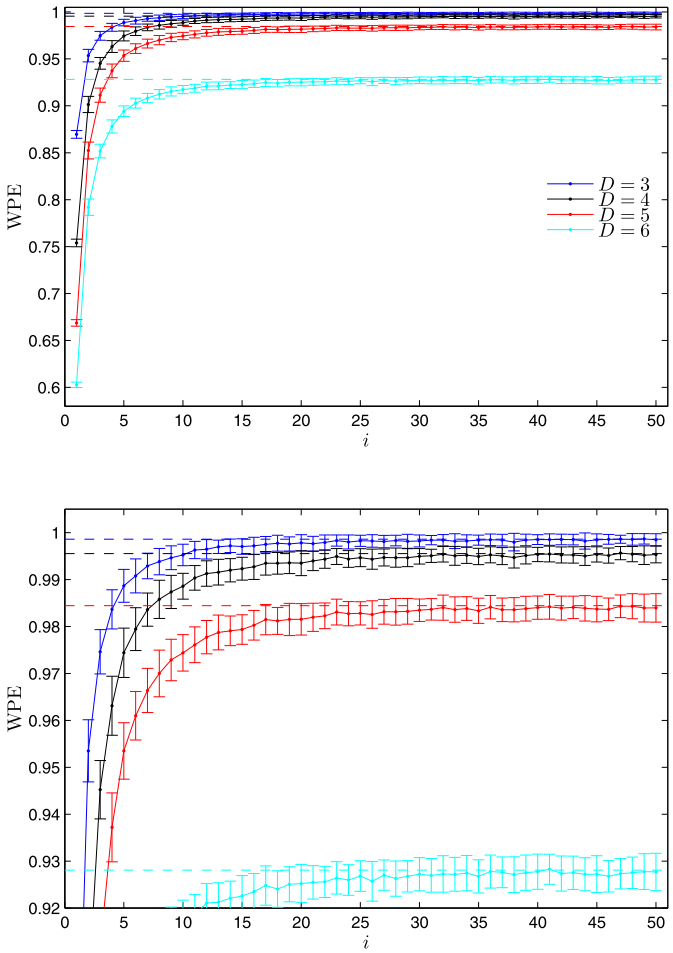

Fig. 3. Same as Fig. 2 but using the normalized WPE, an improved PE better suited to characterize signals having considerable amplitude information [44]. (For interpretation of the references to color in this figure legend, the reader is referred to the web version of this article.)

correctly) the presence of non-trivial dynamics. Interested readers can see these additional results in the Supplementary Material. Finally, it is worth remarking here that the normalized PE and WPE estimated values for numerical realizations of continuous uniformly distributed pseudorandom numbers (horizontal dashed lines in Figs. 2–4) are lower than one due to finite-size effects. The offset increases as a function of the embedding dimension D and it decreases for larger time series lengths.

4. Two simple applications

4.1. Decimal expansion of irrational numbers

As a first application, we are interested to investigate the randomness of the decimal expansion of irrational numbers by using the PE. We analyzed the ordinal pattern probability distribution of the temporal sequences obtained by picking the first 10,000 digits of the decimal expansion of several irrational numbers such as π, e, and $\sqrt{2}$. For illustrative purpose, we have plotted the first one hundred entries of these time series in Fig. 5. The relative frequencies of the ordinal patterns with different embedding dimensions, $D \in \{3, 4, 5, 6\}$, and embedding delay $\tau = 1$ for the sequences associated with these three irrational numbers are shown in Figs. 6–8. Ordinal patterns are numbered following the convention used by Parlitz et al. [57]. Fig. 9 shows the indices associated with the ordinal patterns for $D = 3$ (top) and $D = 4$ (bottom). As it is visually concluded from Figs. 6–8, the different motifs are not equiprobable. Some of them are more probable than others, indicating, apparently, the presence of temporal complex structures in the data. But perhaps what is more intriguing is the fact that the relative frequencies of the ordinal patterns seem to be the same for the different irrational numbers. Consequently, the normalized PE estimated values are very similar as it is detailed in Table 1. Are these irregular ordinal patterns probability distributions due to true temporal correlations or can they be attributed to the occurrence of high frequencies of ties? In order to provide an answer to this question, we estimate the normalized PE of an ensemble of one hundred sequences of $N = 10{,}000$ pseudorandom integer values drawn from a discrete uniform distribution on the interval $[0, 9]$. The relative frequencies of the ordinal patterns for one arbitrarily chosen pseudorandom realization is shown in Fig. 10. It is worth pointing out here the strong similarity with the corresponding relative frequencies of the ordinal patterns obtained for the irrational numbers analysis (please compare Figs. 6–8 with Fig. 10). The mean μ and standard deviation σ of $\mathcal{H}_S$ for the one hundred pseudorandom realizations are detailed in Table 2. These results are consistent with those obtained from the sequences of irrational numbers, *i.e* the normalized PE estimations for π, e, and $\sqrt{2}$ (please see Table 1) lie inside the three standard deviations confidence interval ($\mu \pm 3\sigma$)

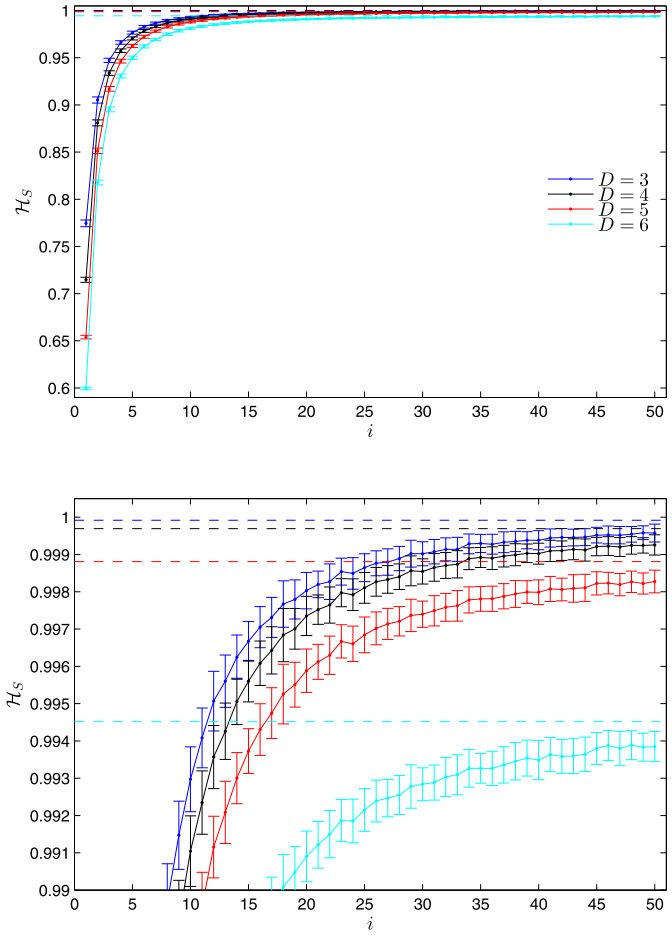

Fig. 4. Same as Fig. 2 but for time series of length $N = 10{,}000$ data points. (For interpretation of the references to color in this figure legend, the reader is referred to the web version of this article.)

Table 1
Normalized PE values for the first 10,000 digits of the decimal expansion of π, e, and $\sqrt{2}$ with different embedding dimensions and embedding delay $\tau = 1$.

	$D = 3$	$D = 4$	$D = 5$	$D = 6$
π	0.992	0.990	0.986	0.978
e	0.992	0.989	0.986	0.978
$\sqrt{2}$	0.992	0.991	0.988	0.980

obtained for the pseudorandom simulations (please see Table 2). Thus, the presence of true temporal correlations should be discarded. We have also carried out a surrogate analysis with shuffled realizations. More precisely, one thousand independent shuffled realizations have been generated for each one of the three irrational sequences. In the shuffled realizations, the values of the original series are simply permuted in a random way. By construction, this procedure generates a time series that preserves the marginal distribution of the original time series but is otherwise independent. Results obtained are summarized in Fig. 11 where boxplots are used to display the distributions of normalized PE estimated values for the shuffled realizations. Since the normalized PE calculated for the original series overlap with those obtained for their shuffled counterparts, this surrogate analysis allows to confirm, once again, that the null hypothesis of randomness can not be rejected. This finding is in agreement with results obtained by Luque et al. [62], who have implemented a totally different (complex network) approach. Our results also imply that the irregularly observed frequency of motifs is a totally spurious effect due to the significant number of equalities that is present in the original

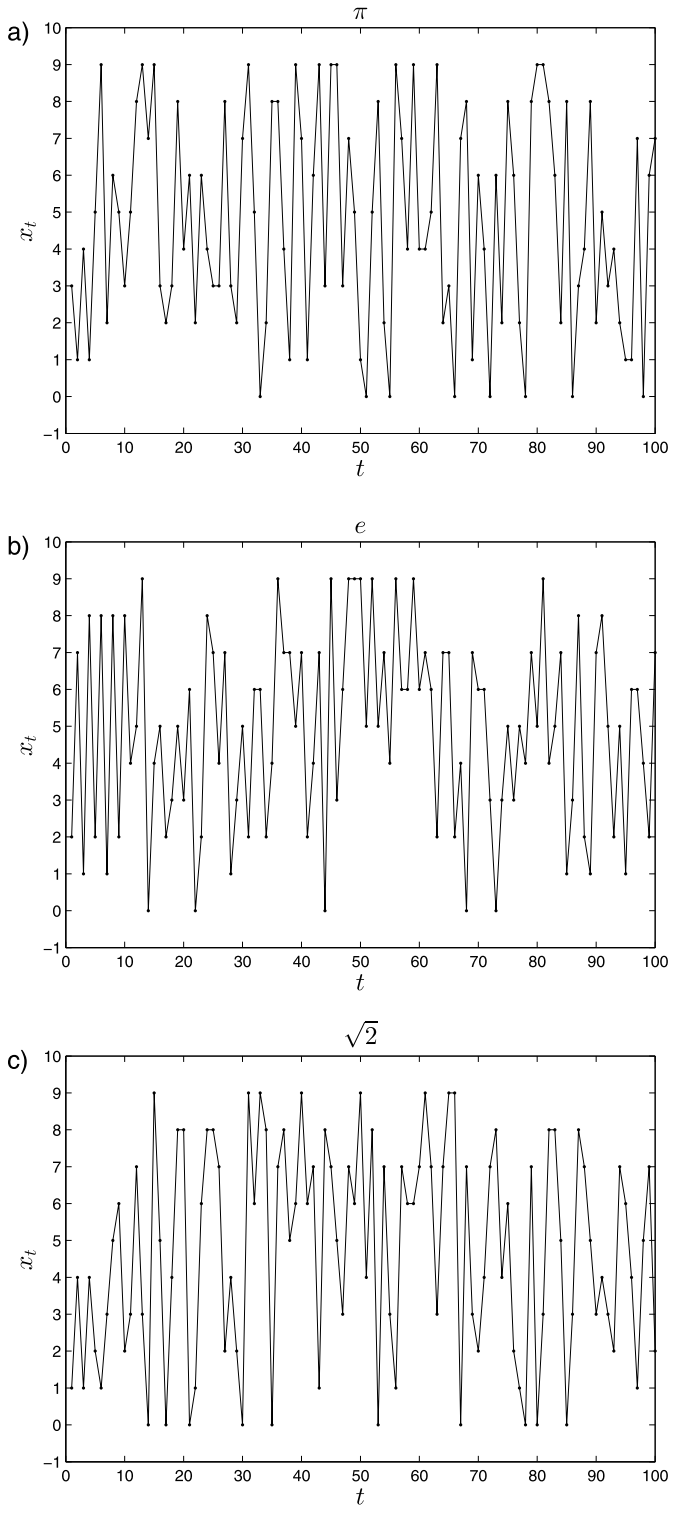

Fig. 5. Sequences of digits associated with the decimal expansion of a) π, b) e, and c) $\sqrt{2}$. Only the first one hundred entries are shown for a better visualization.

time series. Moreover, a surrogate analysis with shuffled realizations appears as a practical alternative to overcome this limitation of the PE.

4.2. Radioactive decay data

We have finally developed an ordinal symbolic analysis for radioactive decay data. Radioactive decay is a widely recognized natural source of random numbers [63,64], whereas subtle long-term

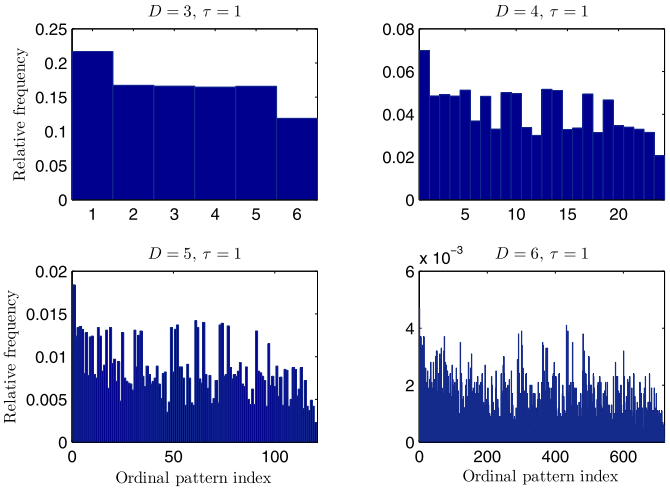

Fig. 6. Relative frequencies of the ordinal patterns for the first 10,000 digits of the decimal expansion of π. Different embedding dimensions, $D \in \{3, 4, 5, 6\}$, and embedding delay $\tau = 1$ have been considered. Indices associated with motifs follow the convention used by Parlitz et al. [57].

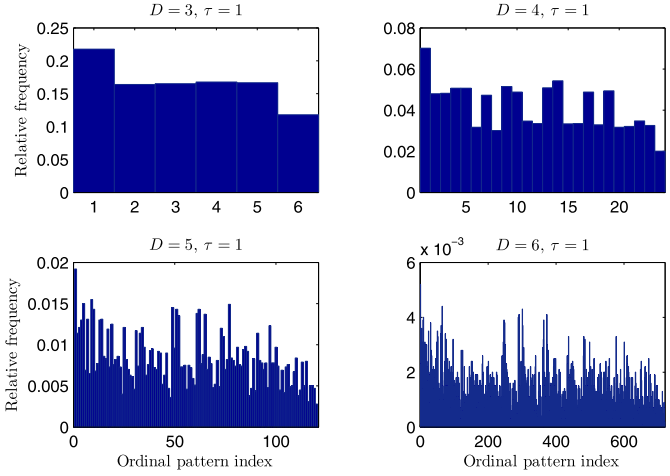

Fig. 7. Same as Fig. 6 but for e.

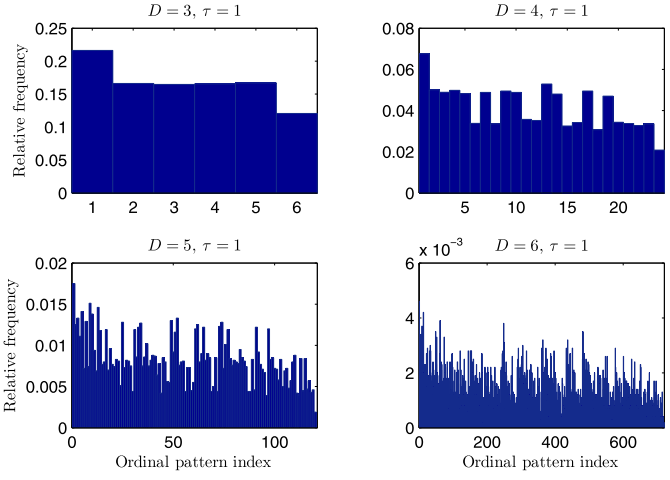

Fig. 8. Same as Fig. 6 but for $\sqrt{2}$.

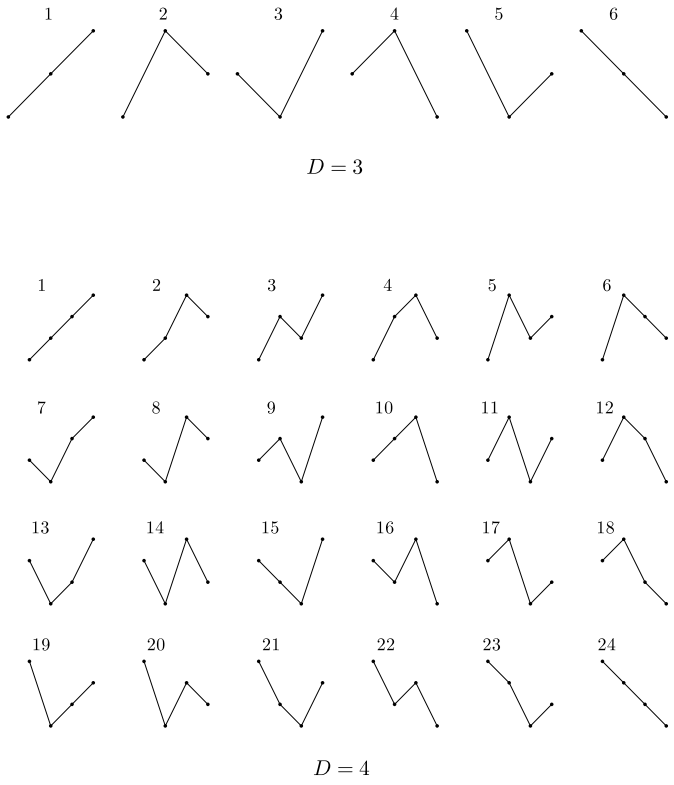

Fig. 9. Ordinal patterns for $D = 3$ (top) and $D = 4$ (bottom) are depicted. They are numbered following the convention used by Parlitz et al. [57].

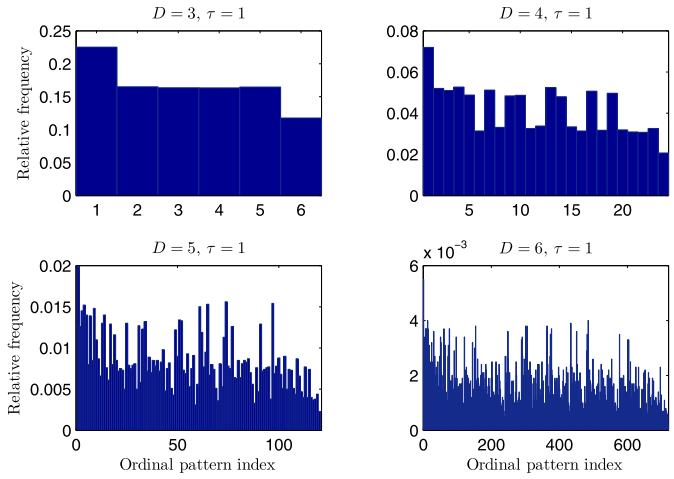

Fig. 10. Same as Fig. 6 but for an arbitrarily chosen sequence of $N = 10{,}000$ pseudorandom integer values drawn from a discrete uniform distribution on the interval $[0, 9]$. Behaviors obtained for the other ninety-nine realizations are very similar.

Table 2
Mean μ and standard deviation σ of $\mathcal{H}_S$ (Eq. (1)) for one hundred sequences of $N = 10{,}000$ pseudorandom integer values drawn from a discrete uniform distribution on the interval $[0, 9]$ with different embedding dimensions and embedding delay $\tau = 1$.

	$D = 3$	$D = 4$	$D = 5$	$D = 6$
μ	0.991	0.989	0.986	0.979
σ	0.001	0.001	0.001	0.001

and short-term deviations from randomness have been reported by several research groups [65,66], however. We tested the alpha-activity of plutonium-239 (^{239}Pu, half-life: 24,110 years) looking for the expected random dynamics. A signal of length $N = 10{,}000$

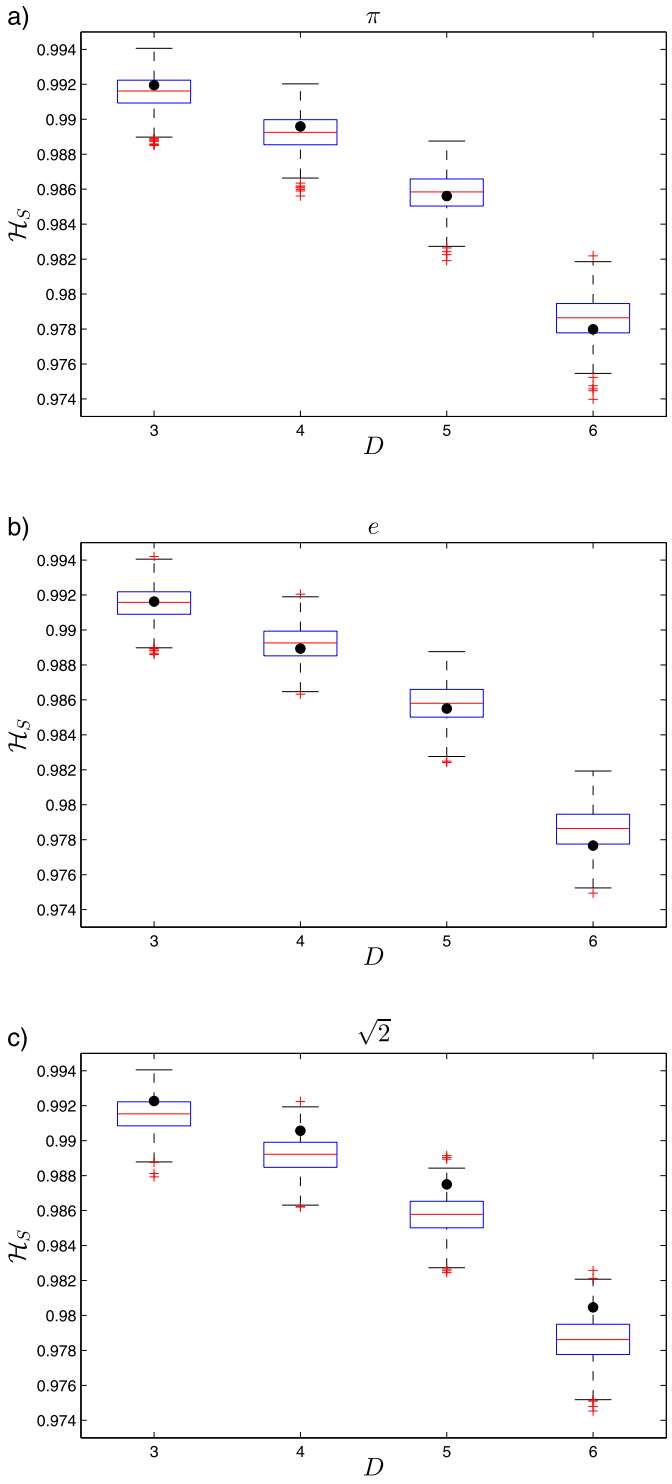

Fig. 11. A surrogate data analysis with one thousand independent shuffled realizations for the first 10,000 digits of the decimal expansion of a) π, b) e, and c) $\sqrt{2}$. The normalized PE (Eq. (1)) has been estimated with different embedding dimensions, $D \in \{3, 4, 5, 6\}$, and embedding delay $\tau = 1$. Black circles indicate the values estimated for the original time series while boxplots are used to display the distributions of estimated values for the shuffled realizations.

(∼2.8 hours) recorded at a sampling rate of 1 Hz by a shielded Geiger counter has been examined. A small segment of the whole record is shown in Fig. 12 and, once again, the occurrence of equalities in the time series is visually verified. The relative frequencies of the ordinal patterns for embedding dimension $D = 3$ and embedding delays τ between 1 and 100 are depicted in Fig. 13a). In

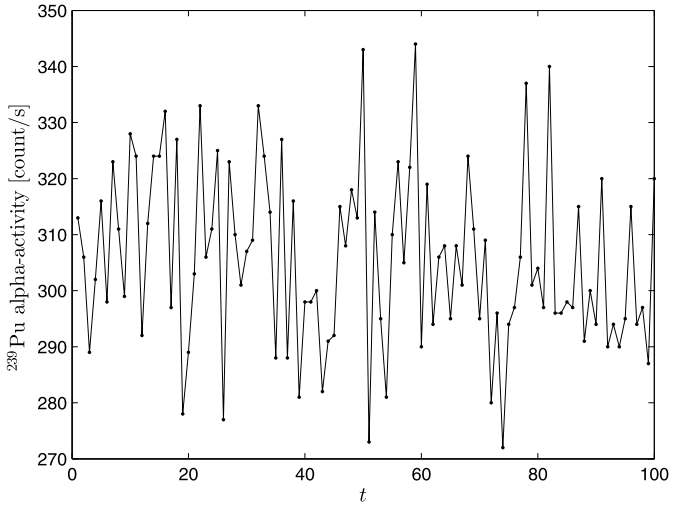

Fig. 12. Alpha-activity of plutonium-239. A small segment of the whole record is shown for a better visualization.

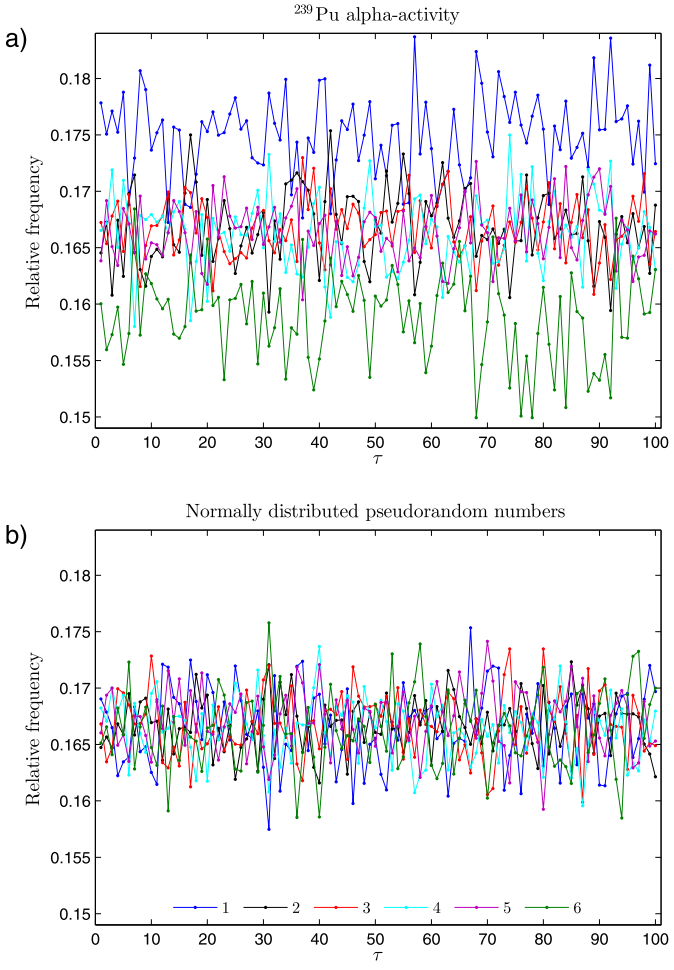

Fig. 13. a) Relative frequencies of the ordinal patterns for the alpha-activity of plutonium-239 with $D = 3$ and $1 \leq \tau \leq 100$. Motifs are labeled following the convention displayed in Fig. 9 (top). b) The same analysis for a sequence of $N = 10{,}000$ normally distributed pseudorandom numbers. (For interpretation of the references to color in this figure legend, the reader is referred to the web version of this article.)

this case we have varied the embedding delay in order to check the behavior of the experimental data for different time scales, *i.e.* for different sampling times. It is concluded that, independently

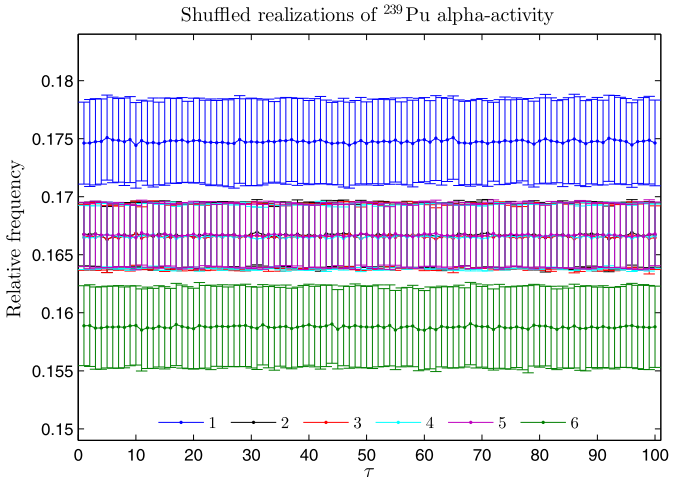

Fig. 14. Relative frequencies of the ordinal patterns for one thousand independent shuffled realizations of the original ^{239}Pu alpha-activity record. Mean and standard deviation (displayed as error bars) of the estimated probabilities with $D = 3$ and $1 \leq \tau \leq 100$ are shown. (For interpretation of the references to color in this figure legend, the reader is referred to the web version of this article.)

of the time scale, the ordinal pattern probability distribution is irregular. In fact, the motif indexed as 1 is clearly more frequent while motif labeled as 6 is less frequent in the temporal sequence. We have also included, in Fig. 13b) and for comparison purpose, the relative frequencies of motifs associated with a sequence of $N = 10{,}000$ normally distributed pseudorandom numbers (by using the *randn* function of MATLAB with the Mersenne Twister generator algorithm). As it was expected, in this continuous case, the six ordinal patterns are equiprobable independently of τ. These results could be taken as an astonishing proof of the presence of non-random structure in radioactive decay. In order to confirm or reject this early interpretation, a similar analysis with one thousand independent shuffled realizations of the original record has been performed. As it is shown in Fig. 14, irregular profiles are also obtained for the shuffled realizations. Hence, the randomness hypothesis can not be rejected. The initial apparent evidence of non-random temporal structure is thus a spurious effect due to the way equal values are handled with the BP algorithm. Although we could not detect non-random behavior in decay data, and our results are in agreement with previous findings about the randomness of radioactive decay [67–71], a non-random behavior of radioactive decay (even in short time-intervals, *i.e.* minutes) were observed by other research groups [65,72–74] employing different data analysis techniques compared to the ones we used. Besides this, our results also not refute the observation of oscillatory [66, 75,76] or transient [77] deviations from the exponential decay in radioactive decay as observed by other studies. The origin of the reported deviations of nuclear decay from randomness is currently controversially discussed in the literature and no final conclusion has been reached.

5. Conclusions

In this paper, we have analyzed the incidence that a significant occurrence of equalities in the time series under study has on PE estimations. Through numerical analysis, it has been shown that PE obtained values are biased as a consequence of the presence of ties in the records. Equal values are usually ranked according to their order of appearance. This way of dealing with ties introduces non-negligible spurious temporal correlations that can potentially lead to erroneous conclusions about the true underlying dynamic nature. Particularly, we have found that lower PE values than those expected are estimated from highly discretized pseudorandom time series. We have also confirmed that experimentally recorded observables digitized with low amplitude resolutions could be especially affected by this PE limitation. Finally, the comparison between the PE calculated from the original time series and the distribution of estimated values from shuffled realizations seems to be a practical and useful strategy to overcome this drawback. Basically, the relative difference between the PE estimated from the original sequence and those values computed from the shuffled realizations should be taken into consideration in order to reliably conclude about the existence of non-trivial temporal dynamics. If the PE associated with the original sequence lies inside the distribution of values estimated from the shuffled counterparts, the null hypothesis that the observed data are temporally uncorrelated can not be rejected. Taking into account that the number of PE applications has increased a lot during the last years, we conjecture that our findings can be of help to reach a more reliable interpretation of results when applying this information-theory-ordinal quantifier to experimentally acquired signals. Furthermore, our results might be also useful when using other quantifiers that implement the BP symbolic representation for characterizing experimental records.

Acknowledgements

We thank Prof. Simon E. Shnoll (Moscow State University, Moscow, and Russian Academy of Sciences, Pushchino) for providing us with the radioactive decay data and Prof. Alejandro Frery (Universidade Federal de Alagoas, Maceió, Alagoas, Brazil) for fruitful discussions about pseudorandom number generators. LZ and OAR gratefully acknowledge financial support from Consejo Nacional de Investigaciones Científicas y Técnicas (CONICET), Argentina. FO thanks support from Pontificia Universidad Católica de Valparaíso.

Appendix A. Supplementary material

Supplementary material related to this article can be found online at http://dx.doi.org/10.1016/j.physleta.2017.03.052.

References

[1] C. Bandt, B. Pompe, Permutation entropy: a natural complexity measure for time series, Phys. Rev. Lett. 88 (17) (2002) 174102, http://dx.doi.org/10.1103/PhysRevLett.88.174102.

[2] Y. Cao, W.W. Tung, J.B. Gao, V.A. Protopopescu, L.M. Hively, Detecting dynamical changes in time series using the permutation entropy, Phys. Rev. E 70 (4) (2004) 046217, http://dx.doi.org/10.1103/PhysRevE.70.046217.

[3] X. Li, G. Ouyang, D.A. Richards, Predictability analysis of absence seizures with permutation entropy, Epilepsy Res. 77 (1) (2007) 70–74, http://dx.doi.org/10.1016/j.eplepsyres.2007.08.002.

[4] X. Li, S. Cui, L.J. Voss, Using permutation entropy to measure the electroencephalographic effects of sevoflurane, Anesthesiology 109 (3) (2008) 448–456, http://dx.doi.org/10.1097/ALN.0b013e318182a91b.

[5] F.C. Morabito, D. Labate, F. La Foresta, A. Bramanti, G. Morabito, I. Palamara, Multivariate multi-scale permutation entropy for complexity analysis of Alzheimer's disease EEG, Entropy 14 (7) (2012) 1186–1202, http://dx.doi.org/10.3390/e14071186.

[6] J. Li, J. Yan, X. Liu, G. Ouyang, Using permutation entropy to measure the changes in EEG signals during absence seizures, Entropy 16 (6) (2014) 3049–3061, http://dx.doi.org/10.3390/e16063049.

[7] Z. Liang, Y. Wang, X. Sun, D. Li, L.J. Voss, J.W. Sleigh, S. Hagihira, X. Li, EEG entropy measures in anesthesia, Front. Comput. Neurosci. 9 (2015) 16, http://dx.doi.org/10.3389/fncom.2015.00016.

[8] F. Montani, R. Baravalle, L. Montangie, O.A. Rosso, Causal information quantification of prominent dynamical features of biological neurons, Philos. Trans. R. Soc. A 373 (2056) (2015) 20150109, http://dx.doi.org/10.1098/rsta.2015.0109.

[9] F. Montani, O.A. Rosso, F.S. Matias, S.L. Bressler, C.R. Mirasso, A symbolic information approach to determine anticipated and delayed synchronization in neuronal circuit models, Philos. Trans. R. Soc. A 373 (2056) (2015) 20150110, http://dx.doi.org/10.1098/rsta.2015.0110.

[10] H. Azami, J. Escudero, Improved multiscale permutation entropy for biomedical signal analysis: interpretation and application to electroencephalogram recordings, Biomed. Signal Process. Control 23 (2016) 28–41, http://dx.doi.org/10.1016/j.bspc.2015.08.004.

[11] M.C. Soriano, L. Zunino, O.A. Rosso, I. Fischer, C.R. Mirasso, Time scales of a chaotic semiconductor laser with optical feedback under the lens of a permutation information analysis, IEEE J. Quantum Electron. 47 (2) (2011) 252–261, http://dx.doi.org/10.1109/JQE.2010.2078799.

[12] L. Zunino, O.A. Rosso, M.C. Soriano, Characterizing the hyperchaotic dynamics of a semiconductor laser subject to optical feedback via permutation entropy, IEEE J. Sel. Top. Quantum Electron. 17 (5) (2011) 1250–1257, http://dx.doi.org/10.1109/JSTQE.2011.2145359.

[13] J.P. Toomey, D.M. Kane, Mapping the dynamic complexity of a semiconductor laser with optical feedback using permutation entropy, Opt. Express 22 (2) (2014) 1713–1725, http://dx.doi.org/10.1364/OE.22.001713.

[14] L. Yang, W. Pan, L. Yan, B. Luo, N. Li, Mapping the dynamic complexity and synchronization in unidirectionally coupled external-cavity semiconductor lasers using permutation entropy, J. Opt. Soc. Am. B 32 (7) (2015) 1463–1470, http://dx.doi.org/10.1364/JOSAB.32.001463.

[15] H. Liu, B. Ren, Q. Zhao, N. Li, Characterizing the optical chaos in a special type of small networks of semiconductor lasers using permutation entropy, Opt. Commun. 359 (2016) 79–84, http://dx.doi.org/10.1016/j.optcom.2015.09.059.

[16] H. Lange, O.A. Rosso, M. Hauhs, Ordinal pattern and statistical complexity analysis of daily stream flow time series, Eur. Phys. J. Spec. Top. 222 (2) (2013) 535–552, http://dx.doi.org/10.1140/epjst/e2013-01858-3.

[17] F. Serinaldi, L. Zunino, O.A. Rosso, Complexity–entropy analysis of daily stream flow time series in the continental United States, Stoch. Environ. Res. Risk Assess. 28 (7) (2014) 1685–1708, http://dx.doi.org/10.1007/s00477-013-0825-8.

[18] T. Stosic, L. Telesca, D.V. de Souza Ferreira, B. Stosic, Investigating anthropically induced effects in streamflow dynamics by using permutation entropy and statistical complexity analysis: a case study, J. Hydrol. 540 (2016) 1136–1145, http://dx.doi.org/10.1016/j.jhydrol.2016.07.034.

[19] P.M. Saco, L.C. Carpi, A. Figliola, E. Serrano, O.A. Rosso, Entropy analysis of the dynamics of El Niño/Southern oscillation during the Holocene, Physica A 389 (21) (2010) 5022–5027, http://dx.doi.org/10.1016/j.physa.2010.07.006.

[20] G. Consolini, P. De Michelis, Permutation entropy analysis of complex magnetospheric dynamics, J. Atmos. Sol.-Terr. Phys. 115–116 (2014) 25–31, http://dx.doi.org/10.1016/j.jastp.2013.11.005.

[21] S. Sippel, H. Lange, M.D. Mahecha, M. Hauhs, P. Bodesheim, T. Kaminski, F. Gans, O.A. Rosso, Diagnosing the dynamics of observed and simulated ecosystem gross primary productivity with time causal information theory quantifiers, PLoS ONE 11 (10) (2016) e0164960, http://dx.doi.org/10.1371/journal.pone.0164960.

[22] L. Zunino, M. Zanin, B.M. Tabak, D.G. Pérez, O.A. Rosso, Forbidden patterns, permutation entropy and stock market inefficiency, Physica A 388 (14) (2009) 2854–2864, http://dx.doi.org/10.1016/j.physa.2009.03.042.

[23] L. Zunino, M. Zanin, B.M. Tabak, D.G. Pérez, O.A. Rosso, Complexity–entropy causality plane: a useful approach to quantify the stock market inefficiency, Physica A 389 (9) (2010) 1891–1901, http://dx.doi.org/10.1016/j.physa.2010.01.007.

[24] A.F. Bariviera, M.B. Guercio, L.B. Martinez, O.A. Rosso, The (in)visible hand in the Libor market: an information theory approach, Eur. Phys. J. B 88 (2015) 208, http://dx.doi.org/10.1140/epjb/e2015-60410-1.

[25] A.F. Bariviera, M.B. Guercio, L.B. Martinez, O.A. Rosso, A permutation information theory tour through different interest rate maturities: the Libor case, Philos. Trans. R. Soc. A 373 (2056) (2015) 20150119, http://dx.doi.org/10.1098/rsta.2015.0119.

[26] R. Yan, Y. Liu, R.X. Gao, Permutation entropy: a nonlinear statistical measure for status characterization of rotary machines, Mech. Syst. Signal Process. 29 (2012) 474–484, http://dx.doi.org/10.1016/j.ymssp.2011.11.022.

[27] A.L.L. Aquino, T.S.G. Cavalcante, E.S. Almeida, A.C. Frery, O.A. Rosso, Characterization of vehicle behavior with information theory, Eur. Phys. J. B 88 (2015) 257, http://dx.doi.org/10.1140/epjb/e2015-60384-x.

[28] A.L.L. Aquino, H.S. Ramos, A.C. Frery, L.P. Viana, T.S.G. Cavalcante, O.A. Rosso, Characterization of electric load with information theory quantifiers, Physica A 465 (2017) 277–284, http://dx.doi.org/10.1016/j.physa.2016.08.017.

[29] F.O. Redelico, F. Traversaro, N. Oyarzabal, I. Vilaboa, O.A. Rosso, Evaluation of the status of rotary machines by time causal information theory quantifiers, Physica A 470 (2017) 321–329, http://dx.doi.org/10.1016/j.physa.2016.05.031.

[30] O.A. Rosso, R. Ospina, A.C. Frery, Classification and verification of handwritten signatures with time causal information theory quantifiers, PLoS ONE 11 (12) (2016) e0166868, http://dx.doi.org/10.1371/journal.pone.0166868.

[31] O.A. Rosso, H.A. Larrondo, M.T. Martín, A. Plastino, M.A. Fuentes, Distinguishing noise from chaos, Phys. Rev. Lett. 99 (15) (2007) 154102, http://dx.doi.org/10.1103/PhysRevLett.99.154102.

[32] L. Zunino, M.C. Soriano, O.A. Rosso, Distinguishing chaotic and stochastic dynamics from time series by using a multiscale symbolic approach, Phys. Rev. E 86 (4) (2012) 046210, http://dx.doi.org/10.1103/PhysRevE.86.046210.

[33] A. Bahraminasab, F. Ghasemi, A. Stefanovska, P.E. McClintock, H. Kantz, Direction of coupling from phases of interacting oscillators: a permutation information approach, Phys. Rev. Lett. 100 (8) (2008) 084101, http://dx.doi.org/10.1103/PhysRevLett.100.084101.

[34] M. Staniek, K. Lehnertz, Symbolic transfer entropy, Phys. Rev. Lett. 100 (15) (2008) 158101, http://dx.doi.org/10.1103/PhysRevLett.100.158101.

[35] L. Zunino, D.G. Pérez, A. Kowalski, M.T. Martín, M. Garavaglia, A. Plastino, O.A. Rosso, Fractional Brownian motion, fractional Gaussian noise, and Tsallis permutation entropy, Physica A 387 (24) (2008) 6057–6068, http://dx.doi.org/10.1016/j.physa.2008.07.004.

[36] X. Zhao, P. Shang, J. Huang, Permutation complexity and dependence measures of time series, Europhys. Lett. 102 (4) (2013) 40005, http://dx.doi.org/10.1209/0295-5075/102/40005.

[37] N. Mammone, J. Duun-Henriksen, T.W. Kjaer, F.C. Morabito, Differentiating interictal and ictal states in childhood absence epilepsy through permutation Rényi entropy, Entropy 17 (7) (2015) 4627–4643, http://dx.doi.org/10.3390/e17074627.

[38] A.M. Unakafov, K. Keller, Conditional entropy of ordinal patterns, Physica D 269 (2014) 94–102, http://dx.doi.org/10.1016/j.physd.2013.11.015.

[39] L. Zunino, F. Olivares, O.A. Rosso, Permutation min-entropy: an improved quantifier for unveiling subtle temporal correlations, Europhys. Lett. 109 (1) (2015) 10005, http://dx.doi.org/10.1209/0295-5075/109/10005.

[40] C. Su, Z. Liang, X. Li, D. Li, Y. Li, M. Ursino, A comparison of multiscale permutation entropy measures in on-line depth of anesthesia monitoring, PLoS ONE 11 (10) (2016), http://dx.doi.org/10.1371/journal.pone.0164104.

[41] F. Olivares, L. Zunino, O.A. Rosso, Quantifying long-range correlations with a multiscale ordinal pattern approach, Physica A 445 (2016) 283–294, http://dx.doi.org/10.1016/j.physa.2015.11.015.

[42] J.P. Toomey, A. Argyris, C. McMahon, D. Syvridis, D.M. Kane, Time-scale independent permutation entropy of a photonic integrated device, J. Lightwave Technol. (2017), http://dx.doi.org/10.1109/JLT.2016.2626387 (in press).

[43] C. Bian, C. Qin, Q.D.Y. Ma, Q. Shen, Modified permutation–entropy analysis of heartbeat dynamics, Phys. Rev. E 85 (2) (2012) 021906, http://dx.doi.org/10.1103/PhysRevE.85.021906.

[44] B. Fadlallah, B. Chen, A. Keil, J. Príncipe, Weighted-permutation entropy: a complexity measure for time series incorporating amplitude information, Phys. Rev. E 87 (2) (2013) 022911, http://dx.doi.org/10.1103/PhysRevE.87.022911.

[45] E.M. Bollt, T. Stanford, Y.-C. Lai, K. Życzkowski, Validity of threshold-crossing analysis of symbolic dynamics from chaotic time series, Phys. Rev. Lett. 85 (16) (2000) 3524–3527, http://dx.doi.org/10.1103/PhysRevLett.85.3524.

[46] J.M. Amigó, K. Keller, V.A. Unakafova, Ordinal symbolic analysis and its application to biomedical recordings, Philos. Trans. R. Soc. A 373 (2034) (2015) 20140091, http://dx.doi.org/10.1098/rsta.2014.0091.

[47] O.A. Rosso, C. Masoller, Detecting and quantifying stochastic and coherence resonances via information-theory complexity measurements, Phys. Rev. E 79 (4) (2009) 040106(R), http://dx.doi.org/10.1103/PhysRevE.79.040106.

[48] O.A. Rosso, C. Masoller, Detecting and quantifying temporal correlations in stochastic resonance via information theory measures, Eur. Phys. J. B 69 (2009) 37–43, http://dx.doi.org/10.1140/epjb/e2009-00146-y.

[49] A. Aragoneses, N. Rubido, J. Tiana-Alsina, M.C. Torrent, C. Masoller, Distinguishing signatures of determinism and stochasticity in spiking complex systems, Sci. Rep. 3 (2013) 1778, http://dx.doi.org/10.1038/srep01778.

[50] A. Aragoneses, T. Sorrentino, S. Perrone, D.J. Gauthier, M.C. Torrent, C. Masoller, Experimental and numerical study of the symbolic dynamics of a modulated external-cavity semiconductor laser, Opt. Express 22 (4) (2014) 4705–4713, http://dx.doi.org/10.1364/OE.22.004705.

[51] A. Aragoneses, L. Carpi, N. Tarasov, D. Churkin, M. Torrent, C. Masoller, S. Turitsyn, Unveiling temporal correlations characteristic of a phase transition in the output intensity of a fiber laser, Phys. Rev. Lett. 116 (3) (2016) 033902, http://dx.doi.org/10.1103/PhysRevLett.116.033902.

[52] D.J. Little, D.M. Kane, Permutation entropy of finite-length white-noise time series, Phys. Rev. E 94 (2) (2016) 022118, http://dx.doi.org/10.1103/PhysRevE.94.022118.

[53] J.A. Reinoso, M.C. Torrent, C. Masoller, Emergence of spike correlations in periodically forced excitable systems, Phys. Rev. E 94 (3) (2016) 032218, http://dx.doi.org/10.1103/PhysRevE.94.032218.

[54] J.A. Reinoso, M.C. Torrent, C. Masoller, Analysis of noise-induced temporal correlations in neuronal spike sequences, Eur. Phys. J. Spec. Top. 225 (13) (2016) 2689–2696, http://dx.doi.org/10.1140/epjst/e2016-60024-6.

[55] A.M. Kowalski, M. Martín, A. Plastino, O.A. Rosso, Bandt–Pompe approach to the classical-quantum transition, Physica D 233 (1) (2007) 21–31, http://dx.doi.org/10.1016/j.physd.2007.06.015.

[56] M. Staniek, K. Lehnertz, Parameter selection for permutation entropy measurements, Int. J. Bifurc. Chaos 17 (10) (2007) 3729–3733, http://dx.doi.org/10.1142/S0218127407019652.

[57] U. Parlitz, S. Berg, S. Luther, A. Schirdewan, J. Kurths, N. Wessel, Classifying cardiac biosignals using ordinal pattern statistics and symbolic dynamics, Comput. Biol. Med. 42 (3) (2012) 319–327, http://dx.doi.org/10.1016/j.compbiomed.2011.03.017.

[58] M. Zanin, L. Zunino, O.A. Rosso, D. Papo, Permutation entropy and its main biomedical and econophysics applications: a review, Entropy 14 (8) (2012) 1553–1577, http://dx.doi.org/10.3390/e14081553.

[59] M. Riedl, A. Müller, N. Wessel, Practical considerations of permutation entropy. A tutorial review, Eur. Phys. J. Spec. Top. 222 (2) (2013) 249–262, http://dx.doi.org/10.1140/epjst/e2013-01862-7.

[60] C. Quintero-Quiroz, S. Pigolotti, M.C. Torrent, C. Masoller, Numerical and experimental study of the effects of noise on the permutation entropy, New J. Phys. 17 (2015) 093002, http://dx.doi.org/10.1088/1367-2630/17/9/093002.

[61] M. Matsumoto, T. Nishimura, Mersenne twister: a 623-dimensionally equidistributed uniform pseudo-random number generator, ACM Trans. Model. Comput. Simul. 8 (1) (1998) 3–30, http://dx.doi.org/10.1145/272991.272995.

[62] B. Luque, L. Lacasa, F. Ballesteros, J. Luque, Horizontal visibility graphs: exact results for random time series, Phys. Rev. E 80 (4) (2009) 046103, http://dx.doi.org/10.1103/PhysRevE.80.046103.

[63] F. James, A review of pseudorandom number generators, Comput. Phys. Commun. 60 (3) (1990) 329–344, http://dx.doi.org/10.1016/0010-4655(90)90032-V.

[64] P.E. Rapp, A.M. Albano, I.D. Zimmerman, M.A. Jiménez-Montaño, Phase-randomized surrogates can produce spurious identifications of non-random structure, Phys. Lett. A 192 (1) (1994) 27–33, http://dx.doi.org/10.1016/0375-9601(94)91010-3.

[65] V.A. Namiot, S.E. Shnoll, On the possible mechanism of periodicity in fine structure of histograms during nuclear decay processes, Phys. Lett. A 359 (4) (2006) 249–251, http://dx.doi.org/10.1016/j.physleta.2006.05.094.

[66] P.A. Sturrock, E. Fischbach, J. Jenkins, Analysis of beta-decay rates for Ag108, Ba133, Eu152, Eu154, Kr85, Ra226, and Sr90, measured at the Physikalisch-Technische Bundesanstalt from 1990 to 1996, Astrophys. J. 794 (1) (2014) 42, http://dx.doi.org/10.1088/0004-637X/794/1/42.

[67] M.P. Silverman, W. Strange, C.R. Silverman, T.C. Lipscombe, Tests of alpha-, beta-, and electron capture decays for randomness, Phys. Lett. A 262 (4–5) (1999) 265–273, http://dx.doi.org/10.1016/S0375-9601(99)00668-4.

[68] M.P. Silverman, W. Strange, C. Silverman, T.C. Lipscombe, Tests for randomness of spontaneous quantum decay, Phys. Rev. A 61 (4) (2000) 042106, http://dx.doi.org/10.1103/PhysRevA.61.042106.

[69] M.P. Silverman, W. Strange, Experimental tests for randomness of quantum decay examined as a Markov process, Phys. Lett. A 272 (1–2) (2000) 1–9, http://dx.doi.org/10.1016/S0375-9601(00)00374-1.

[70] M.P. Silverman, W. Strange, Search for correlated fluctuations in the β^+ decay of Na-22, Europhys. Lett. 87 (3) (2009) 32001, http://dx.doi.org/10.1209/0295-5075/87/32001.

[71] M.P. Silverman, Search for anomalies in the decay of radioactive Mn-54, Europhys. Lett. 114 (6) (2016) 62001, http://dx.doi.org/10.1209/0295-5075/ 114/62001.

[72] S.E. Shnoll, V.A. Kolombet, E.V. Pozharskii, T.A. Zenchenko, I.M. Zvereva, A.A. Konradov, Realization of discrete states during fluctuations in macroscopic processes, Phys. Usp. 41 (10) (1998) 1025–1035, http://dx.doi.org/10.1070/PU1998v041n10ABEH000463.

[73] S.E. Shnoll, E.V. Pozharski, T.A. Zenchenko, V.A. Kolombet, I.M. Zvereva, A.A. Konradov, Fine structure of distributions in measurements of different processes as affected by geophysical and cosmophysical factors, Phys. Chem. Earth (A) 24 (8) (1999) 711–714, http://dx.doi.org/10.1016/S1464-1895(99)00103-9.

[74] V. Milián-Sánchez, A. Mocholí-Salcedo, C. Milián, V.A. Kolombet, G. Verdú, Anomalous effects on radiation detectors and capacitance measurements inside a modified Faraday cage, Nucl. Instrum. Methods Phys. Res. A 828 (2016) 210–228, http://dx.doi.org/10.1016/j.nima.2016.05.051.

[75] P.A. Sturrock, E. Fischbach, J.D. Scargle, Comparative analyses of Brookhaven National Laboratory nuclear decay measurements and Super-Kamiokande solar neutrino measurements: neutrinos and neutrino-induced beta-decays as probes of the deep solar interior, Sol. Phys. 291 (12) (2016) 3467–3484, http://dx.doi.org/10.1007/s11207-016-1008-9.

[76] H. Schrader, Seasonal variations of decay rate measurement data and their interpretation, Appl. Radiat. Isot. 114 (2016) 202–213, http://dx.doi.org/10.1016/j.apradiso.2016.05.001.

[77] T. Mohsinally, S. Fancher, M. Czerny, E. Fischbach, J.T. Gruenwald, J. Heim, J.H. Jenkins, J. Nistor, D. O'Keefe, Evidence for correlations between fluctuations in ^{54}Mn decay rates and solar storms, Astropart. Phys. 75 (2016) 29–37, http://dx.doi.org/10.1016/j.astropartphys.2015.10.007.